

Investigation of the Synthesis and Characterization of Novel Graphene Nanoplatelets (GNPs)

Rajiv Kumar¹, Monika¹, Yogesh Kumar Saini¹, Renu Sharma², and Mamraj Singh*¹

¹*Department of Physics, University of Rajasthan, Jaipur, India.*

¹*Department of Physics, JECRC University, Jaipur, India*

**Corresponding Author E-mail:bmamrajsingh@gmail.com*

Abstract: This study investigates the synthesis and characterization of GNPs. X-ray diffraction (XRD) confirmed that the GNPs exhibit crystallinity, with an average crystallite size of approximately 10 nm, suggesting around 30 graphene layers. Raman spectroscopy and high-resolution transmission electron microscopy (HRTEM) shows the multilayered structure of the GNPs, with lateral dimensions in the micron range. These findings highlight the potential applications of GNPs in energy storage, sensor technologies, and electronics.

Introduction

Graphene is an important material due to its outstanding properties, such as high electrical conductivity, excellent mechanical strength, and thermal stability [1-6]. Among the various graphene-based structures, graphene nanoplatelets (GNPs) have emerged as highly promising due to their unique combination of desirable properties and practical features[2]. It comprising multiple graphene layers (~10 nm thick) in 1 to 50 μm lateral dimension [7].

GNPs retain much of the remarkable functionality of graphene while exhibiting enhanced structural characteristics, including

improved mechanical strength and a large surface area with light weight [7-11]. Due to its Cost effective synthesis and multiple layers structure make useful to make noval nonocomposite with various materials [9,11-13]. These attributes make GNPs well-suited for use in energy storage, sensors, electronics, and composite materials. [8, 12-13].

The synthesis of GNPs generally focuses on controlling factors such as layer number, particle size, and surface properties to optimize their performance for various applications [2,7]. The electronic and mechanical properties of GNPs are highly influenced by structural characteristics such as crystallinity, layer stacking, and defect density[7-11]. GNPs can be synthesized through methods like liquid exfoliation[14,15], the reduction [16] or vapour phase [17], with each technique offering specific advantages in terms of scalability, quality, and cost. XRD and Raman spectroscopy are commonly employed to assess these structural features, helping to determine the degree of exfoliation and presence of defects [18-19].

This study is to investigate the synthesis, structural characterization, surface morphology, and optical properties of GNPs. This comprehensive analysis will contribute to a deeper understanding of structural features and functional performance, ultimately guiding the development of GNPs.

Materials and Methods

Synthesis of Graphene Nanoplatelets

To synthesize graphene nanoplatelets, an 8 mL solution was prepared by combining fuming sulfuric acid (20%) (*Sigma-Aldrich*) with 98% sulfuric acid (*Loba Chemie, India*) in a 1:1 ratio. It was cool to room temperature. Next, 1.0 g of $(\text{NH}_4)_2\text{S}_2\text{O}_8$ (*Sigma-Aldrich*) was gradually introduced to the acid solution while stirring continuously. After stirring about 6 minutes, 0.1 g of flake graphite (*Sigma-Aldrich*) was added. The solution was swirled until a deep-blue color appeared. After 200 minutes, the reaction was then quenched with water, followed by filtration and washing with water and air-dried for 30 hours [20-21].

Characterization Techniques

The XRD pattern was obtained using a Panalytical X'Pert Pro diffractometer with a $\text{Cu-K}\alpha$ radiation source ($\lambda = 1.5418 \text{ \AA}$). For surface morphology a Tecnai G2 20 S-[FEI] TWIN HRTEM was used. The Raman spectrum was recorded with a Confocal Laser Raman spectrometer (LabRAM HR800), with a 532 nm wavelength laser.

Result and discussion

Structural Characterization

Figure 1, illustrates the XRD pattern of graphene nanoplatelets, recorded over a 2θ

range of 10° to 70° . The observed diffraction peak at $\sim 26.6^\circ$, which corresponds to the (002) crystal plane of graphene[7]. An inset in **Figure 1** displays a Lorentzian line shape fit applied to the experimental data to the (002) peak with $R^2 = 0.97$, allowing for calculation of the peak positions. It also gives the full width at half maximum (FWHM, B_{hkl}).

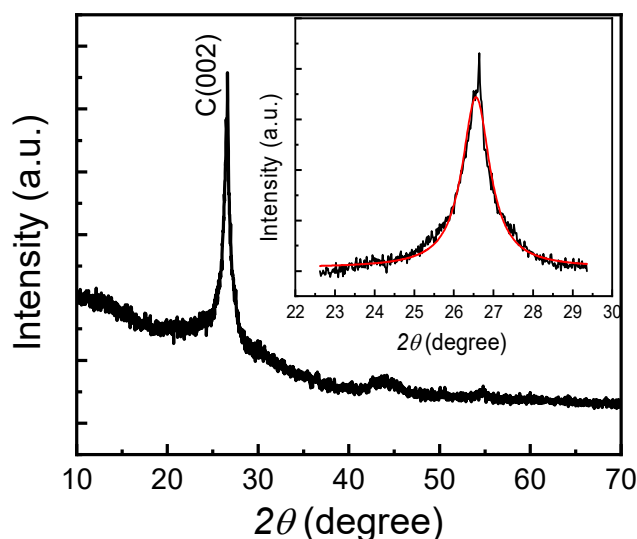


Figure 1: XRD pattern of GPNs recorded over a 2θ range of 10° to 70° . The inset (red line) shows the Lorentzian line shape fit to the (002) peak with $R^2 = 0.97$.

The interlayer spacing between adjacent graphene sheets was calculated based on the first-order diffraction ($n=1$) from the (002) plane, using Bragg's law:

$$\lambda = 2 d_{002} \sin\theta \quad (1)$$

where d_{hkl} is the interlayer distance, and θ is the Bragg angle. For X-ray wavelength (λ) of 0.154 nm, the calculated interlayer distance d_{002} is $\sim 0.335 \text{ nm}$ [14].

To estimate the crystallite size along the $\langle 002 \rangle$ direction, we applied the Scherrer equation [22]:

$$D_{hkl} = 0.9 \lambda / B_{hkl} \cos \theta \quad (2)$$

where D_{hkl} is the crystallite size, $FWHM$ of the diffraction peak in radians.

Using this equation (2), with a Bragg angle of 13.3° and the X-ray wavelength (0.154 nm), we calculated the crystallite size along the $\langle 002 \rangle$ direction to be approximately 10 nm . This crystallite size suggests the presence of around 30 graphene monolayers stacked in the $\langle 002 \rangle$ orientation.

Surface Morphology

The HRTEM images (see figure 2) show that the GNPs exhibit a well-defined, layered structure with lateral sizes extending into the micron range. The lateral size, extending over microns, suggests that the GNPs could provide extensive surface area which is beneficial for applications in devices and sensors, [12-13].

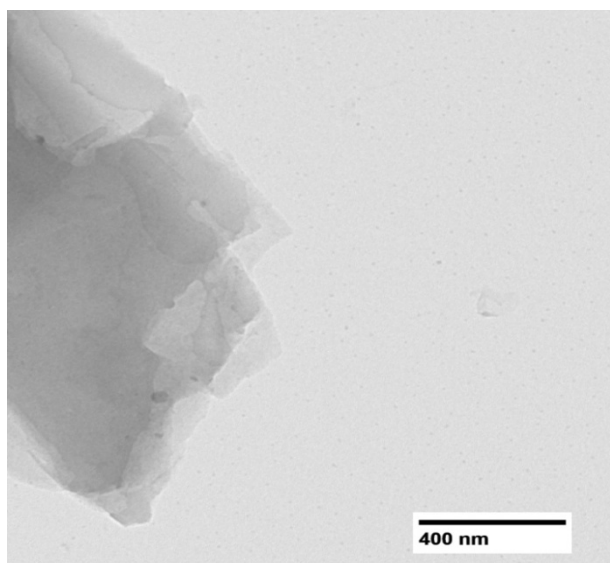
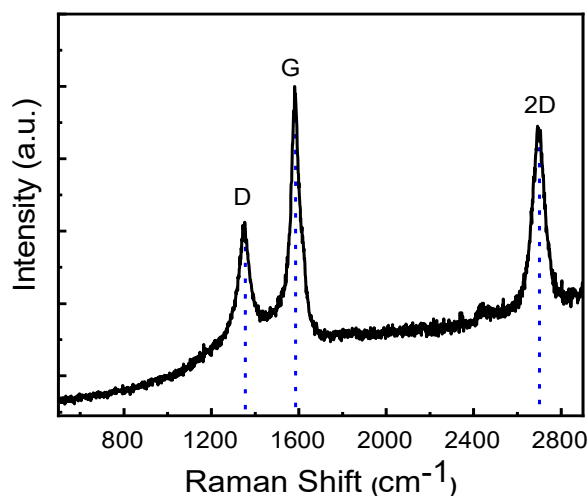


Figure 2: HRTEM image of GNPs showing a lateral size in the micron range.

Optical Properties

Figure 3(a) shows Raman spectrum of graphene nanoplatelets, displaying the characteristic Raman features of the G band, D band, and 2D band [23]. Lorentzian line shape fit to the Raman spectrum of graphene nanoplatelets (see Figure 3(b)), yielding an R^2 value of 0.98, indicating a high-quality fit. Analysis of the fitting parameters reveals D peak, G peak and 2D peak position occurs at 1349 cm^{-1} , 1582 cm^{-1} , and 2696 cm^{-1} respectively [23-24].

The G peak, located at 1582 cm^{-1} , corresponds to the in-plane vibration of sp^2 -bonded carbon atoms, signifying graphitic structure[23]. The D peak, centered at 1349 cm^{-1} , is corresponding breathing mode of carbon ring[23]. This mode activated due to defect in ring. Therefore it indicates the presence of structural imperfections within the carbon atoms ring. The 2D peak, observed at 2696 cm^{-1} , results from as an overtone of the D band (two photon scattering), further confirming the graphitic nature of the sample.



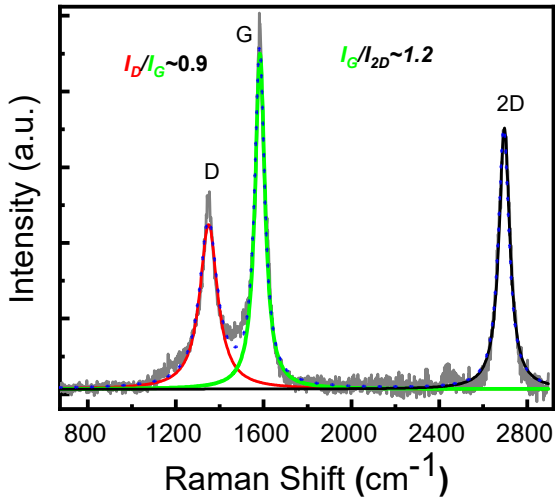


Figure 3: (a) Raman spectrum of graphene nanoplatelets. (b) Raman spectrum with Lorentzian line shape fitting applied, showing peaks at 1349 cm^{-1} , 1582 cm^{-1} , and 2696 cm^{-1} . The calculated intensity ratios, $I_D/I_G \approx 0.9$ and $I_G/I_{2D} \approx 1.2$. An R^2 value of 0.98 confirms a high-quality fit.

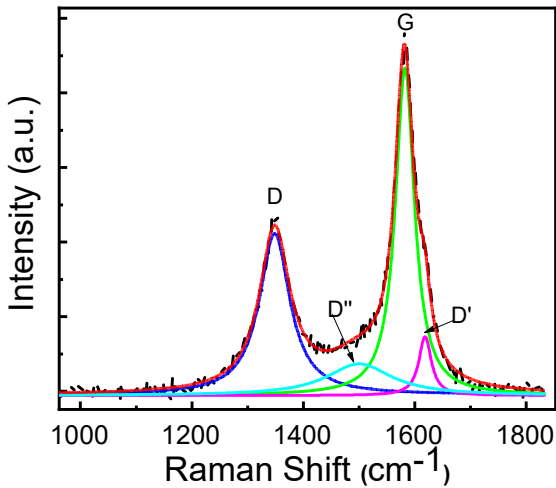


Figure 4: Raman spectra for the D band and G band of GNPs. Lorentzian line shape fitting applied to identify characteristic peaks, including the D band ($\sim 1349\text{ cm}^{-1}$), D' band ($\sim 1618\text{ cm}^{-1}$), D'' band ($\sim 1500\text{ cm}^{-1}$), and G band ($\sim 1582\text{ cm}^{-1}$). The R^2 value of 0.99 indicates an excellent fit.

The intensity ratios $I_D/I_G \approx 0.9$ and $I_G/I_{2D} \approx 1.2$ suggest that the sample consists of multilayered graphene (also defects) with an estimated layer count of approximately 30, consistent with the findings from XRD analysis [25].

Figure 4 presents the Raman spectra of GNPs, highlighting the D and G bands. Further analysis using the Lorentzian line shape fitting reveals four distinct peaks corresponding to the D ($\sim 1349\text{ cm}^{-1}$), D' ($\sim 1618\text{ cm}^{-1}$), D'' ($\sim 1500\text{ cm}^{-1}$), and G ($\sim 1582\text{ cm}^{-1}$) bands, with an R^2 value of 0.99 indicating an excellent fit [25]. The detailed fitting parameters, including intensity and FWHM, are presented in Table 1.

Table 1: Fitting parameters obtained from Lorentzian line shape fitting of the Raman spectra of graphene nanoplatelets (Figure 4).

S. No	Raman Shift (cm^{-1})	A (Area)	w (cm^{-1})
D	1349.1 ± 0.3	452130	66.4 ± 0.9
G	1582.3 ± 0.1	568512	4141.2 ± 0.6
D''	1500.1 ± 3.4	189269	141.9 ± 12.5
D'	1618.4 ± 0.6	66608	2726.9 ± 1.9

From Table 1, we can see that beside the D peak at 1349 cm^{-1} , and G peak at 1582 cm^{-1} , we have additional peaks. The D'' peak at 1500 cm^{-1} , a second-order defect band with lower intensity and a broader width of 142 cm^{-1} , implies more complex or dispersed defects [23-25]. The D' band at 1618 cm^{-1} , with the lowest

intensity and narrowest width (27 cm^{-1}), indicates fewer defects in this mode [25].

Overall, the Raman data reveal a balance between graphitic ordering (G band) and varying degrees of disorder (D, D', and D'' bands), affecting the material's electronic and mechanical properties, with narrower peaks suggesting fewer or more localized defects.

Conclusion

The synthesis and characterization of GNPs reveal their high crystalline and multilayered structure. XRD and HRTEM confirm the GNPs' excellent structural integrity, while Raman analysis shows a balance of graphitic order and defects. These findings suggest that GNPs are well-suited for sensors and devices.

References

- [1] Novoselov, K. S., Geim, A. K., Morozov, S., Jiang, D., Zhang, Y., Dubonos, S. A., Grigorieva, I., & Firsov, A. (2004). Electric field effect in atomically thin carbon films. *Science*, *306*(5696), 666–669.
- [2] Bunch, J. S., Van Der Zande, A. M., Verbridge, S. S., Frank, I. W., Tanenbaum, D. M., Parpia, J. M., Craighead, H. G., & McEuen, P. L. (2007). Electromechanical resonators from graphene sheets. *Science*, *315*(5811), 490–493.
- [3] Katsnelson, M. I. (2007). Graphene: Carbon in two dimensions. *Materials Today*, *10*(1-2), 20–27.
- [4] Kopelevich, Y., & Esquinazi, P. (2007). Graphene: A system with unusual electronic properties. *Advanced Materials*, *19*(26), 4559–4563.
- [5] Morozov, S., Novoselov, K., Katsnelson, M., Schedin, F., Elias, D., Jaszczak, J., & Geim, A. (2008). Giant intrinsic carrier mobilities in graphene and its bilayer. *Physical Review Letters*, *100*(1), 016602.
- [6] Becerril, H. A., Mao, J., Liu, Z., Stoltenberg, R. M., Bao, Z., & Chen, Y. (2008). Evaluation of solution-processed reduced graphene oxide films as transparent conductors. *ACS Nano*, *2*(3), 463–470.
- [7] Wick, P., Louw-Gaume, A. E., Kucki, M., et al. (2014). Classification framework for graphene-based materials. *Angewandte Chemie International Edition*, *53*(27), 7714–7718.
- [8] Nag, A., Simorangkir, R. V. B., Gawade, D. R., et al. (2022). Graphene-based wearable temperature sensors: A review. *Materials & Design*, *221*, 110971.
- [9] Akm, A. I., Clement, S. H., Mainul, H. (2024). Graphene (GNP) reinforced 3D printing nanocomposites: An advanced structural perspective. *Heliyon*, *10*, e28771.
- [10] Ahmed, A. (2023). Mechanical characterization of graphene nanoparticles. In Abdellaoui, H., et al. *Mechanics of Nanomaterials and Polymer Nanocomposites*. Springer, Singapore.
- [11] Jain, V., Jaiswal, S., Dasgupta, K., & Lahiri, D. (2024). Fabrication of GNPs sprayed carbon fiber and its effects on the interfacial and mechanical behavior of reinforced epoxy multiscale laminated composite. *Polymer Composites*.
- [12] Ganesan, S., Muthuraj, A., Dhanabalan, K., et al. (2024). Recent progress using

- graphene oxide and its composites for supercapacitor applications: A review. *Inorganics*.
- [13]Prabhu, L., Saravanan, R., Anderson, A., et al. (2023). Synthesis, thermal adsorption, and energy storage calibration of polysulfone nanocomposite developed with GNP/CNT nanofillers. *Adsorption Science & Technology*.
- [14]Ji, S., Park, L., Lee, C. S., et al. (2014). Liquid-phase exfoliation of expanded graphites into graphene nanoplatelets using amphiphilic organic molecules. *Journal of Colloid and Interface Science*.
- [15]Nguyen, T. A., Nguyen, T. T., Phuong, N. T. H., & Bhosale, S. V. (2018). Study on industrial-scale fabrication of graphene nanoplatelets (GNPs) from natural graphite. *Materials Science Forum*.
- [16]Singh, R. K., Singh, D. P., & Singh, R. K. (2016). Graphene oxide: strategies for synthesis, reduction and frontier applications. *RSC Advances*, 6(69), 64993–65011.
- [17]Chinke, S. L., Gawade, R., & Alegaonkar, P. S. (2019). Synthesis and characterization of graphene-like nano flakes (GNF) using chemical vapor deposition. *AIP Conference Proceedings*.
- [18]Huh, S. H. (2014). X-ray diffraction of multi-layer graphenes: Instant measurement and determination of the number of layers. *Carbon*, 78, 617–621.
- [19]Graf, D., Molitor, F., Ensslin, K., et al. (2007). Spatially resolved Raman spectroscopy of single- and few-layer graphene. *Nano Letters*, 7(2), 238–242.
- [20]Dimiev, A. M., Ceriotti, G., Metzger, A., et al. (2016). Chemical mass production of graphene nanoplatelets in ~100% yield. *ACS Nano*.
- [21]La, Y. D., Bhargava, S. K., & Bhosale, S. V. (2016). Improved and simple approach for mass production of graphene nanoplatelets material. *ChemistrySelect*.
- [22]Scherrer, P. (1918). Bestimmung der Größe und der inneren Struktur von Kolloidteilchen mittels Röntgenstrahlen. *Göttinger Nachrichten Math. Phys.*, 2, 98–100.
- [23]Malard, L. M., Pimenta, M. A., Dresselhaus, G., & Dresselhaus, M. S. (2009). Raman spectroscopy in graphene. *Physics Reports*, 473(5–6), 51–87.
- [24]Ferrari, A. C., & Robertson, J. (2000). Interpretation of Raman spectra of disordered and amorphous carbon. *Physical Review B*, 61, 14095–14107.
- [25]Ferrari, A. C., Meyer, J. C., Scardaci, V., et al. (2006). Raman spectrum of graphene and graphene layers. *Physical Review Letters*, 97, 187401.